Journal of Solid State Chemistry 184 (2011) 2668–2677

Contents lists available at ScienceDirect

Journal of Solid State Chemistry

journal homepage: www.elsevier.com/locate/jssc

Decomposition of molybdate–hexamethylenetetramine complex: One single source route for different catalytic materials

Sandra Chouzier [a], Tivadar Czeri [b], Magalie Roy-Auberger [b], Christophe Pichon [b], Christophe Geantet [a], Michel Vrinat [a], Pavel Afanasiev [a,*]

[a] Institut de recherches sur la catalyse et l'environnement de Lyon UMR5256, CNRS-Université de Lyon 1, 2 avenue Albert Einstein, 69626 Villeurbanne cedex, France
[b] IFP Energies nouvelles, BP 3, 69390 Vernaison, France

ARTICLE INFO

Article history:
Received 9 June 2011
Received in revised form
1 August 2011
Accepted 7 August 2011
Available online 11 August 2011

Keywords:
Molybdenum
Nitride
Sulfide
Catalyst
Hexamethylenetetramine

ABSTRACT

Decomposition of ammonium heptamolybdate–hexamethylentetramine (HMTA) complex $(HMTA)_2(NH_4)_4Mo_7O_{24}\cdot 2H_2O$ was studied as a function of treatment conditions in the range 300–1173 K. The evolution of solid products during decomposition was studied by thermal analysis and in situ EXAFS. Depending on the nature of the gas used for treatment, single phases of highly dispersed nitrides Mo_2N, carbide Mo_2C, or oxide MoO_2 can be obtained. The nature of the products obtained was explained by qualitative thermodynamical considerations. Morphology of the solids considerably depends on such preparation parameters as temperature and mass velocity of the gas flow. For the nitride-based materials, catalytic activity was evaluated in the model thiophene HDS reaction. It was demonstrated that NH_3-treated samples showed better catalytic activity than N_2-treated ones due to cleaner surface and better morphology. Transmission microscopy, XRD and XPS studies showed that MoS_2 is formed on the surface during HDS reaction or sulfidation with H_2S. Optimized nitride-derived catalysts showed mass activity several times higher than unsupported MoS_2 or MoS_2/Al_2O_3 reference catalyst.

1. Introduction

Transition metals nitrides and carbides are important inorganic materials with widespread range of applications, extending from superconductivity to highly resistant alloys and catalysis. Since the temperature-programmed reaction method was first applied [1–3] to synthesize unsupported Mo_2N and Mo_2C with high specific surface areas, a number of reactions including hydrodesulfurization (HDS) and hydrodenitrogenation (HDN) [4–6], hydrogenation [7,8], ammonia synthesis [9,10] and hydrodeoxygenation [11] reactions have been studied over this type of catalysts, including monometallic or bimetallic nitrides and carbides [12]. Unsupported nitride and carbide materials as well as supported on alumina or zeolites [13] were extensively studied. To improve the textural properties of inorganic nitrides, alternative preparation methods have been proposed such as sonochemical technique [14], laser-promoted nitridation [15] or carbothermal route [16].

Recently we developed an original technique for the preparation of highly dispersed Mo_2N by decomposition of molybdate hexamethylenetetramine (HMTA) precursor [17]. HMTA molecule served at once as a source of nitrogen and as a reducing agent to remove oxygen in the form of carbon oxides. This approach was further applied to prepare bulk and supported bimetallic molybdenum nitrides with cobalt or nickel [18–20], supported nitride materials [21], metals [22] or molybdenum phosphide [23]. Though highly divided nitride was prepared by this technique, further optimization of such preparations in scope of catalytic applications was still possible. Moreover we observed that the results of preparations depend on several parameters, including the crystallinity of the precursor or the value of gas flow mass velocity. Sometimes considerable amounts of MoO_2 impurity were found in the solid products, depending on the drying conditions applied prior to the thermal treatment. Moreover, a non-intuitive dependence of the product composition on the gas composition was observed. Thus, carbide Mo_2C was observed if the reaction was carried out in hydrogen. To explain these findings and to prepare highly active unsupported catalysts, the present study has been undertaken.

2. Experimental

2.1. Preparation of solids

HMTA complex was obtained by an aqueous reaction of ammonium heptamolybdate and HMTA as described in [17]. Decomposition was carried out in a quartz reactor under nitrogen,

* Corresponding author. Fax: +33 04 72 44 53 99.
E-mail address: pavel.afanasiev@ircelyon.univ-lyon1.fr (P. Afanasiev).

0022-4596/$ - see front matter © 2011 Elsevier Inc. All rights reserved.
doi:10.1016/j.jssc.2011.08.005

ammonia or hydrogen flow, with a rate 5 K min^{-1}. In some experiments the gas flow was saturated by water vapor at 273 K (0.6 kPa pressure). The solids were kept and handled under inert atmosphere. Sulfidation was carried out in a flow of 15% H_2S/H_2 mixture at 673 K for 4 h.

2.2. Characterizations

X-ray diffraction patterns were obtained on a Bruker diffractometer with Cu $K\alpha$ emission. The diffractograms were analyzed using the standard ICSD files. Chemical analyses were realised using the atomic emission method. Surface areas and pore radii distributions were measured by low temperature nitrogen adsorption and calculated using BET, BJH or Horvath-Kawazoe [24] equations. The Mo content in the solids was analyzed by plasma coupled atomic emission spectroscopy (AES-ICP-Horiba Jobin Yvon). The amounts of carbon, hydrogen, nitrogen and sulfur (CHNS) in the solids were determined on a EA1110-CHNS device. Scanning electron microscopy images were obtained on a Hitachi S800 device at CMEABG center of Lyon Claude Bernard University. Transmission electron micrographs were obtained on a JEOL 2010 device with an accelerating voltage of 200 KeV. The X-ray photoelectron spectroscopy (XPS) experiments were carried out with a KRATOS AXIS Ultra DLD spectrometer using a hemispherical analyzer and working at a vacuum higher than 10^{-9} mbar. All the data were acquired using monochromatic Al $K\alpha$ X-rays (1486.6 eV, 150 W), a pass energy of 20 eV, and a hybrid lens mode. The analyzed area was 700 μm × 300 μm. Charge neutralization was carried out for all samples. The adventitious carbon (C1s=284.5 eV) was taken as internal reference. The chemical state has been evaluated by curve fitting in the Mo 3*d*, O 1*s* and S 2*p* regions using a minimum number of doublets.

Thermal analysis experiments were carried out on a SETARAM, Setsys Evolution 12 device, coupled to a PFEIFFER Omnistar 2006 mass-spectrometer. The gaseous products evolved upon heating of the samples were studied using electron impact energy of 65 eV. The samples were heated in a platinum crucible at a rate of 5 K min^{-1} from 298 to 1173 K.

EXAFS measurements were carried out at the X1 beamline of HASYLAB synchrotron facility. In situ measurements were carried out in an in situ cell used previously in [25] and adopted from [26], represented in Fig. 1. The measurements were carried out in transmission mode at the Mo *K* edge (20,000 eV) at ambient temperature, with 2 eV step, 2 s per point. The sample thickness was chosen to give an absorption edge step of about 1.0. Phase shifts and backscattering amplitudes were obtained from FEFF [27] calculations on model compounds. The EXAFS data were treated with VIPER program [28]. Curve fitting was done alternatively in *R* and *k* space and the fit was accepted only in the case of simultaneous convergence (absolute and imaginary parts for the *R*-space). Coordination numbers (CN), interatomic distances (*R*), Debye–Waller parameters (σ^2), and energy shifts (ΔE_0) were used as fitting variables. Constraints were introduced, relating the fitting parameters in order for them to have the values lying in physically reasonable intervals. Comparison between the models depending on different number of parameters was performed on the basis of *F*-test.

2.3. Catalytic tests

Thiophene HDS tests were carried out without exposure to oxygen, the nitrides were prepared directly in the catalytic reactor. A weighted amount of precursor was introduced into the catalytic reactor. The precursor was decomposed under nitrogen or ammonia flow at 823–1023 K. Then the reactor was filled with argon, closed and transferred to the catalytic test and heated to 613 K with a rate 10 K min^{-1} under the flow of hydrogen saturated with thiophene. After 12 h on stream the temperature began to vary between 573 and 613 K in order to measure kinetics and to build Arrhenius's plot of the reaction rate. The properties of the solid catalysts were determined after the catalytic test. The products were analyzed using on-line gas chromatography. Reaction rate was determined using pseudo-first rate equation assuming a large excess of hydrogen and relatively low conversion (0.1 or lower).

3. Results and discussion

3.1. Composition and properties of solid products as a function of treatment conditions

The initial complex has chemical composition $(C_6H_{12}N_4)_2(NH_4)_4Mo_7O_{24}\cdot 2H_2O$ (**I**). This compound was precipitated and characterized earlier but we have not succeeded to grow its monocrystals suitable for structure determination. Preliminary characterizations suggested that in this compound the $Mo_7O_{24}^{6-}$ ions are preserved but NH_4^+ ions are partially substituted by protonated HTMA cations.

Decomposition of **I** under non-reactive N_2 or Ar flow led to dispersed Mo_2N, as described previously [17]. However in the course of more detailed study we observed that fine details of treatment conditions might be important. Thus, the size of crystals of **I** influences the composition of the product. Indeed, if precipitation of **I** was carried out under vigorous stirring, octahedral particles were obtained with size 10 μm (Fig. 2a), which decompose in N_2 always leading to some MoO_2 impurity. By contrast, large crystals (50 μm and more) of the same compound obtained without stirring (Fig. 2b) led to pure Mo_2N phase. This suggested that the nature of decomposition product is somewhat borderline, and even slight variations of treatment conditions are

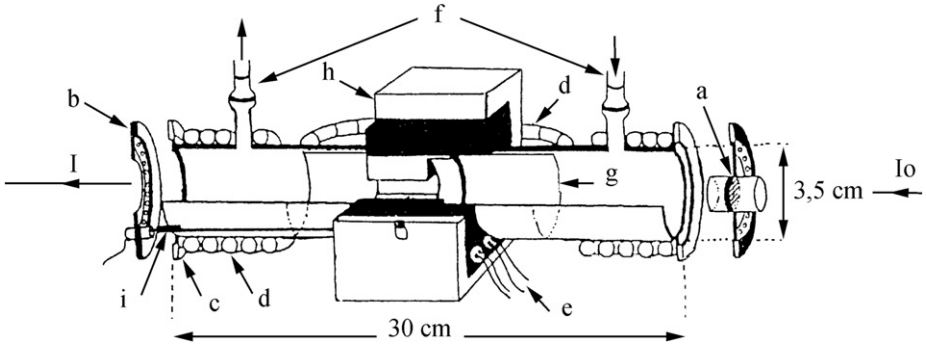

Fig. 1. In situ cell for transmission EXAFS experiments: a—quartz sample holder; b—Kapton windows; c—joints; d—cooling circuit; e—heating elements; f—gas entries; g—quartz tube; and h—furnace.

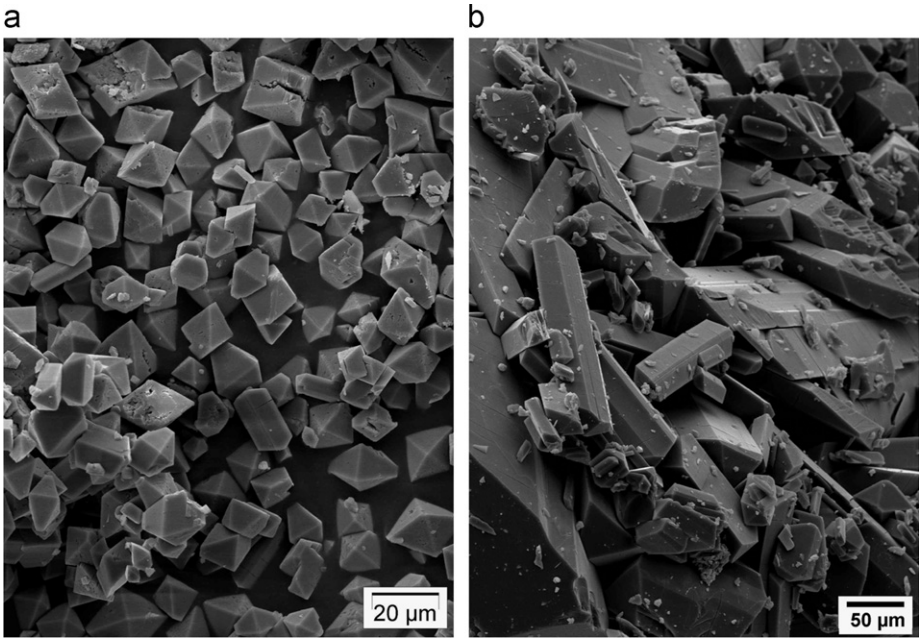

Fig. 2. SEM photographs of crystallites of the compound **I** obtained by precipitation without stirring (a) and with stirring at 60 s^{-1} rate (b). The initial solids have identical composition and XRD patterns, but decompose differently under N_2 flow (see text).

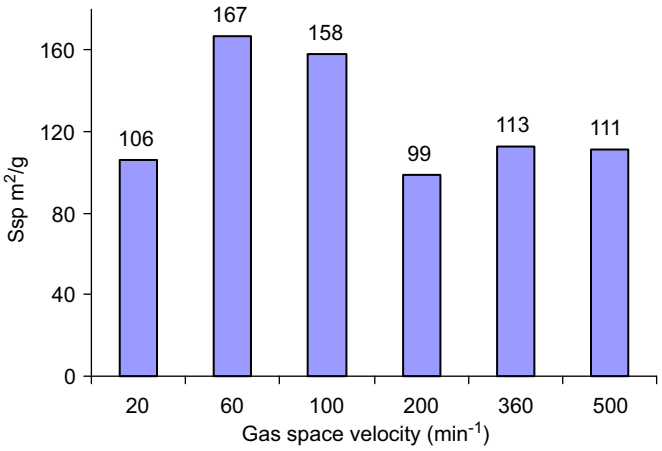

Fig. 3. Influence of nitrogen space velocity on the specific surface area of Mo_2N materials obtained from the decomposition of **I** at 923 K.

prone to modify the product. Moreover, the mass flow of N_2 substantially influenced the textural properties of the solids. The dependence of the specific surface area on the nitrogen flow velocity is represented in Fig. 3. It shows that the textural parameters of the materials obtained vary significantly and attain an optimum at intermediate values of flow rate.

The importance of crystal size and gas flow velocity for the properties of decomposition product indicated that the instant local concentration of gaseous reaction products in the decomposition zone might play considerable role. As was observed previously, water and ammonia are the main products of decomposition of HMTA complexes, as well as carbon oxides and some H_2. Therefore, we studied the influence of gas atmosphere in a more controllable manner introducing water vapor and/or NH_3 in the gas flow. Our practical goal was to optimize the preparation technique in view of catalytic applications.

We observed that decomposition in wet N_2 yielded pure MoO_2 phase with very low Ssp (Table 1). By contrast, if aqueous ammonia was applied to saturate the flowing gas, pure Mo_2N was obtained, though its Ssp was much lower as compared to the samples prepared under dry conditions. These findings can be explained from simple considerations based on Le Châtelier's principle. Indeed, water is a product of oxygen removal from the precursor, whereas ammonia can be formed from the reductive decomposition of nitride. Therefore addition of water and NH_3 to the gas flow favours, respectively, formation of MoO_2 and Mo_2N. Note that addition of water can change the nature of the products of reductive decomposition and make appear MoO_2 in the reactions of molybdates. Thus reduction of $NiMoO_4$ in wet hydrogen leads to MoO_2–Ni mixture, whereas reduction in dry H_2 produces Ni–Mo alloy [29].

Table 1
Phase composition and specific surface area (Ssp) of the decomposition products (923 K) of complex **I** as a function of the flowing gas composition.

Gas composition	Product, DRX phases	Ssp, (m^2/g)
N_2	Mo_2N	145
NH_3	Mo_2N+β-Mo_2N[a]	175
H_2	Mo_2C	5
H_2, 603 Pa H_2O	Mo_2C	<1
3% H_2 in Ar	Mo_2C	50
N_2, 603 Pa H_2O	MoO_2	<1
N_2 saturated by NH_3.aq	Mo_2N	33

[a] Impurity of the second polymorph, less than 10% vol. The main product is always γ-Mo_2N.

Less obviously, decomposition under pure H_2 or in 5% H_2–N_2 mixture led invariably to pure Mo_2C phase. In pure H_2, Mo_2C carbide with low Ssp was obtained (Table 1). This carbide product forms large crystals with the size greater than the initial **I** compound (Fig. 4). Diluting of hydrogen allowed a considerable increase of Ssp to several tens of square meters per gram, but pure Mo_2C remained the only product.

Finally, using NH_3 flow led to highly divided materials consisting of the mixture of γ-Mo_2N and impurity β-Mo_2N phases and having small particles of ca 3–5 nm size (Fig. 5a). Under the same conditions decomposition in N_2 flow led to a sponge-like and more agglomerated material (Fig. 5b). The Ssp values of

NH_3-treated specimens were higher than reported earlier for Mo_2N obtained under nitrogen or inert gas flow (Table 1). Remarkably, using NH_3 flow yielded pure and crystallized Mo_2N material at the temperature as low as 823 K (Fig. 6a), the lowest temperature ever reported for this material synthesis. Heating under nitrogen required higher temperature to crystallize Mo_2N and was prone to form MoO_2 impurity (Fig. 6b).

We can conclude that decomposition of complex **I** produces versatile materials. The best textural properties were obtained if the decomposition was assisted with NH_3. Worth noting that

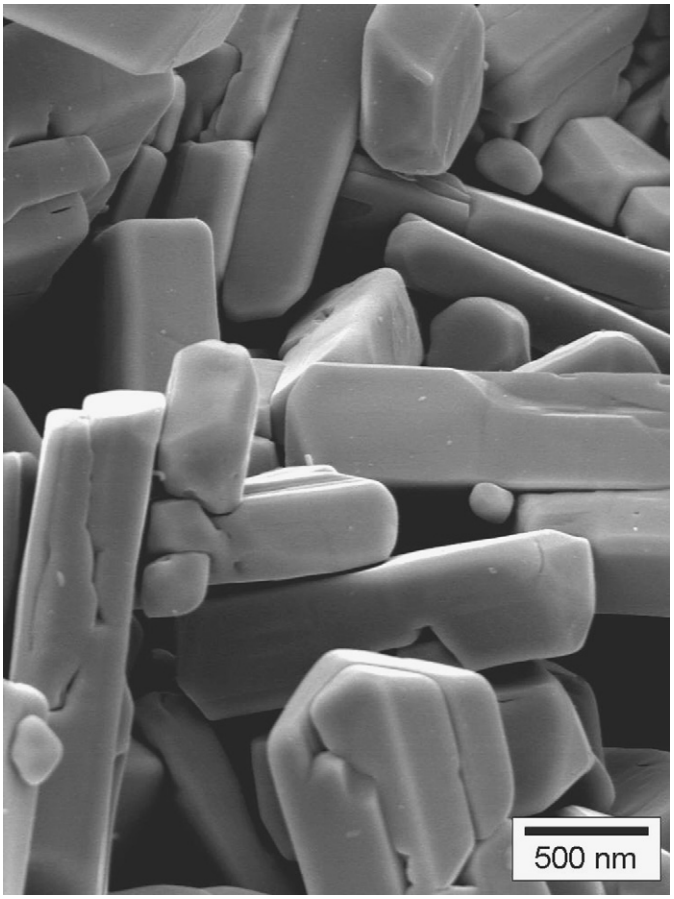

Fig. 4. SEM image of molybdenum carbide crystals, obtained by decomposition of **I** at 1073 K in flowing hydrogen.

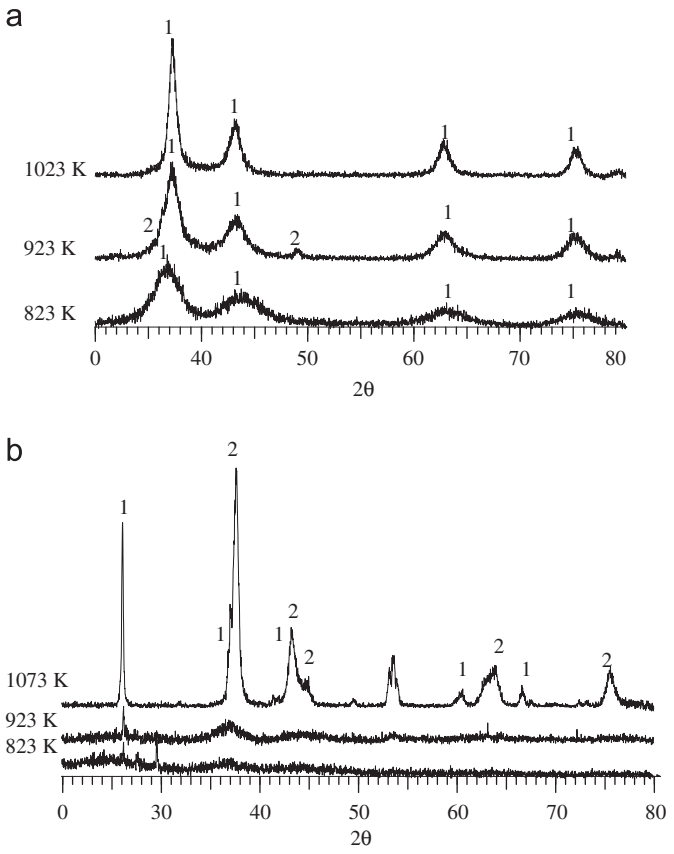

Fig. 6. XRD patterns of the decomposition products of **I** obtained by precipitation with stirring, after heating in NH_3 (a) and in N_2 (b). Peaks marks: for (a): 1—γ-Mo_2N, 2—β-Mo_2N; for (b): 1–γ-Mo_2N, 2–MoO_2.

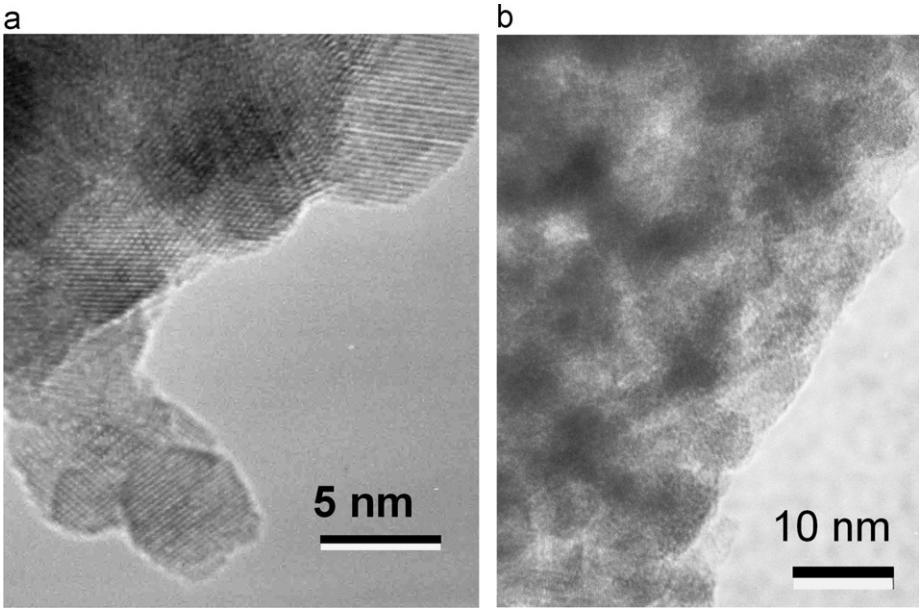

Fig. 5. TEM images ot the solids prepared at 923 K under NH3 (a) and under N_2 flow (b).

formation of dispersed nitride under NH_3 flow was achieved at much lower temperatures (823 K) than for temperature programmed reaction of oxide precursors in NH_3. It appears that nitrogen, water or ammonia do not directly react with the solids but just change the equilibrium conditions for the evolution of common precursor (vide infra). As with hydrogen, it does not noticeably react up to 673 K, and then it probably withdraws oxygen from the intermediate solid products, which explains Mo_2C formation. Indeed, in the absence of oxygen in the intermediate decomposition product of composition MoC_xN_y, carbon would not be able to leave as CO or CO_2, still nitrogen would be able to leave as N_2. By this obvious reason, further high temperature evolution favours formation of Mo_2C. These qualitative speculations are further supported by physical characterisations, thermal analysis and in situ EXAFS.

Remarkably, chemical composition of all samples heated at 673 K was similar, whatever the gas applied (Table 2). Only at 773 K the compositions diverged as a function of gas atmosphere. Higher nitrogen contents and lower residual carbon amounts were observed at equal temperatures in the NH_3- treated samples, than in the N_2-treated ones, while in both cases progressive evolution to nitride occurred. For the H_2-treated solids, an intermediate carbide–nitride composition was formed at 773 K, which rapidly lost nitrogen at higher temperatures, yielding virtually pure carbide.

3.2. Thermal analysis

In the TGA–MS experiments, heating in argon (instead of nitrogen) was carried out as a case study of decomposition in a non-reactive gas, because this allowed observation of the $m/z=28$ species (N_2, CO). We observed earlier that decomposition of **I** under nitrogen and argon flow give quite similar results. Diluted gas flow containing 5% vol. H_2 in Ar was applied to study decomposition towards carbide. The corresponding curves are presented in Figs. 7 and 8, respectively, for treatment under inert and hydrogen flow. The results of TGA in ammonia were not sound because at low temperatures NH_3 signal strongly interfered with those of the decomposition products whereas at higher temperatures catalytic decomposition of NH_3 occurred, screening other processes. Thermal analysis coupled with mass-spectrometry showed that the main decomposition events occur below 673 K whatever the gas atmosphere. After 673 K smooth decomposition continued without appearance of any sharp peaks neither in the mass loss nor in thermal events.

Decomposition of **I** to carbide and to nitride both give theory loss weight of ca. 52.5%, which is close to observed at 1100 K values of 52%. Two endothermic mass losses (10.5wt% in total) at 390 and 450 K are related to the dehydration and the loss of ammonia. Dehydration of **I** may account for only 2.5% weight loss, whereas the loss of ammonia with simultaneous production of one water molecule per two ammonia molecules represents 7.5% mass loss. Then, sharp exothermal decomposition peak at 520 K appeared, with additional 10wt% mass loss. This peak might correspond to a redox reaction of HMTA with heptamolybdate species. After the exothermic peak, more smooth mass loss occurred without any noticeable thermal events. Decomposition continued up to 1020 K and resulted in the total weight loss well corresponding to the removal of all light elements from the compound **I**, leaving only Mo_2N or Mo_2C. The decomposition under 5% H_2–Ar proceeded with the same dehydration steps as in nitrogen, but the exothermal peak at 520 K was less pronounced than under nitrogen, though the mass loss at this point was the same. In both cases NH_3 release gave the most intense events with a main peak near 450 K. Then, the second peak of NH_3 release at 510–520 K was accompanied by formation of CO_2 and an exothermal effect. Further heating produced CO_2 and (CO, N_2) signals smeared over a wide range of temperature. Overall, no striking differences between TGA and MS curves were observed for two cases (compare Figs. 7 and 8). This similarity of MS and TGA curves between the processes leading, respectively, to carbide and nitride shows that in a great extent both processes are governed by the relatively low-temperature decomposition step, occurring below 673 K.

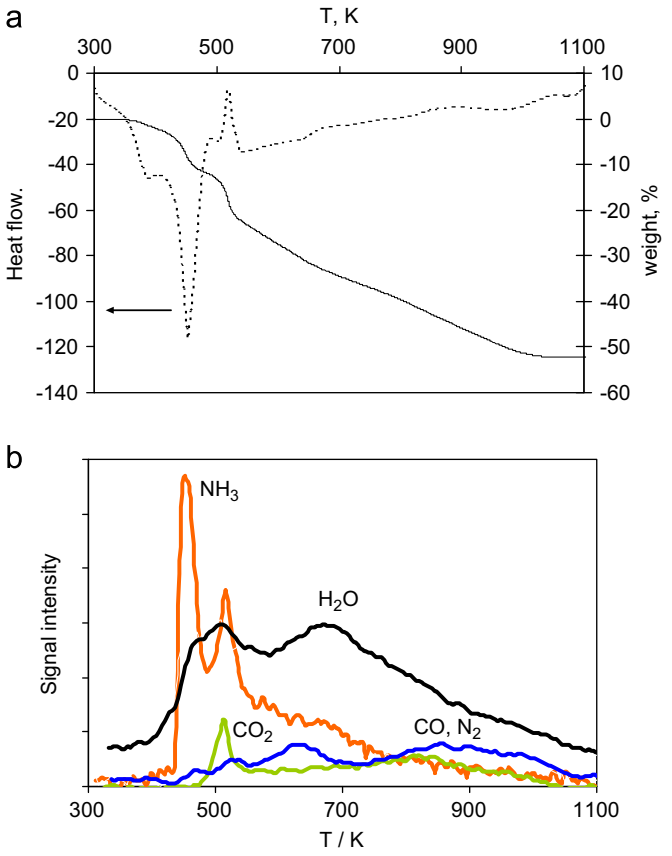

Fig. 7. Thermal analysis (a) and mass-spectrometry of evolved gases (b) during decomposition of **I** decomposition under flowing argon.

Table 2
Chemical composition of **I** decomposition products as a function of temperature and the nature of gas flow.

T (K)	N_2	NH_3	H_2
673	$Mo_2N_{1.30}C_{1.44}$	$Mo_2N_{1.47}C_{0.98}$	$Mo_2N_{1.24}C_{1.32}$
773	$Mo_2N_{1.15}C_{0.86}$	$Mo_2N_{1.45}C_{0.26}$	$Mo_2N_{0.41}C_{1.10}$
823	$Mo_2N_{0.93}C_{0.61}$	$Mo_2N_{1.48}C_{0.08}$	$Mo_2N_{0.13}C_{0.99}$
923	$Mo_2N_{0.8}C_{0.16}$	$Mo_2N_{1.32}C_{0.06}$	$Mo_2N_{0.07}C_{0.91}$
1073	$Mo_2N_{0.81}C_{0.06}$	$Mo_2N_{1.14}C_{0.016}$	$Mo_2N_{0.02}C_{0.85}$

3.2.1. In situ EXAFS study

In situ EXAFS study was carried out to have an idea about structural evolution of the solids while they remain amorphous, i.e. below 823 K. The samples treated in N_2 and NH_3 were compared as presenting more interest for their further use in catalysis. The results obtained in these two gases were similar and here we discuss only NH_3 treated solids supposing that the same discussion is valid for nitrogen-treated ones, unless otherwise stated. In situ Mo K edge EXAFS allowed observing coordination of Mo in the amorphous state as a function of temperature.

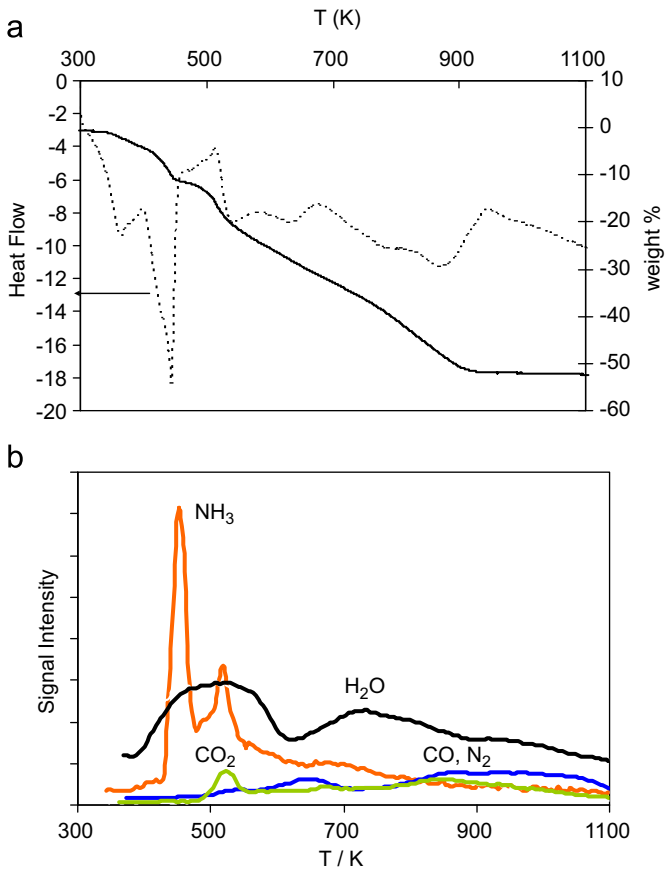

Fig. 8. Thermal analysis (a) and mass-spectrometry of evolved gases (b) during decomposition of **I** decomposition under flowing mixture 5% vol. H_2–Ar.

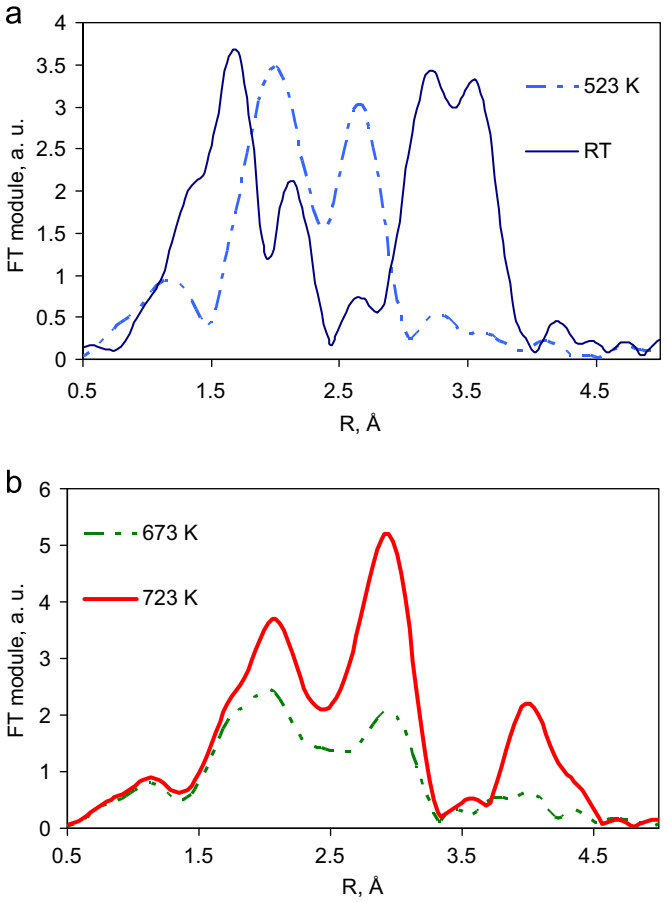

Fig. 9. Fourier transforms of Mo K edge EXAFS spectra of **I** decomposition under nitrogen flow at progressively increasing temperatures.

Unfortunately due to the closeness of carbon, nitrogen and oxygen masses, the light elements in the coordination sphere of molybdenum could not be distinguished. However we observed the evolution of the interatomic distances and CN in the first and the second coordination shells, which provides a valuable information.

As already mentioned, the structure of compound **I** was not resolved. However, from the comparison with ammonium heptamolybdate, it follows that the $Mo_7O_{24}^{6-}$ entities are preserved in **I**, since the XAS spectra of two compounds were virtually identical. Fig. 9 represents Fourier transforms of the EXAFS spectra measured at different temperatures. Between room temperature and 423 K, no strong change of the first coordination shell occurred, but only some slight reorganization in the Mo–Mo shell (3.2–3.8 Å), related probably to some transformation of the polyoxometalate species caused by dehydration (not shown). The breakthrough occurred at 523 K, i.e immediately after the exothermal event in TGA, when the intensity of Mo–Mo scattering drastically dropped and its maximum shifted to lower distances (Fig. 9a). Simultaneously, at 523 K the peak corresponding to the short Mo═O double bonds (1.6–1.8 Å) decreased in intensity, whereas that of longer single Mo–O bonds (2.1–2.3 Å) increased. At the same time, a peak at 2.67 Å appeared, suggesting creation of some metal–metal bonds. Therefore, already at 523 K collapse of polyoxometallate structure occurred with the formation of reduced species. Note that at 523 K the second neighbor distances are smaller than the Mo–Mo distances in Mo_2N (2.93 Å) and correspond rather to the Mo–Mo bonds in the reduced Mo oxides (e.g. 2.51 Å in MoO_2). The whole picture of coordination change correspond to the transition from the Mo_7O_{24} species containing corner and edge-staring MoO_6 octahedra (distorted due to second order Jahn–Teller effect), towards more symmetric face-sharing MoO_6 units in a reduced oxide. At the same time the total intensity of the signal decreased, indicating disordering. Therefore, consistently with formation of carbon oxides observed in TGA–MS, auto reduction of **I** occurred in the range of temperatures 500–600 K. Note that auto-reduction is not a specific feature of HMTA complexes. Indeed, formation of reduced oxides upon decomposition of ammonium heptamolybdate in inert atmosphere was previously reported [30].

The shift of the Mo–Mo bond distance towards 2.9 Å region characteristic for Mo_2N commenced at 673 K and became well pronounced at 723 K (Fig. 9b). At this temperature, the spectrum corresponded to finely divided (and disordered) Mo_2N solid. Numeric data on the distances and coordination numbers (CN) in the decomposition products are presented in Table 3. Note that for well defined crystalline **I** (or ammonium heptamolybdate, having the same spectrum) the average CN values are obtained from the fitting procedure, which do not directly correspond to real crystallographic values. In such crystalline compounds the EXAFS-derived CN values are decreased as compared to the theory values due to the negative interference of scattering from the oxygen neighbors in highly distorted MoO_6 octahedra, having unequal distances (as discussed e.g. in [31] for a similar case of thiomolybdates). Worth emphasizing also that the positions of FT maxima in the lumps of peaks composed by signals from two or more scatteres having close but different distances might be placed rather far from the corresponding true distances, due to the phase interference.

In the amorphous compounds due to the static disorder, the inequality of interatomic distances is even greater than in the crystals. Therefore the apparent CN values become even lower.

Table 3
EXAFS fit parameters for the solids obtained from the decomposition of **I**.

T (K)	Atom	*d* (Å)	CN[a]	DW (Å^2)	Δ*E* (eV)
N_2 flow					
298	O	1.82	3.3	0.005	0.9
	O	2.14	1.4	0.006	0.8
	Mo	3.15	1.3	0.006	0.9
	Mo	3.50	1.6	0.006	0.9
423	O	1.87	3.1	0.006	−0.5
	O	2.14	1.6	0.007	−0.5
	Mo	3.40	2.1	0.006	0.8
523	N(O,C)	2.00	2.1	0.006	0.5
	N(O,C)	2.11	2.4	0.007	0.4
	Mo	2.58	1.0	0.008	0.9
673	N(O,C)	2.04	2.9	0.01	−1.0
	Mo	2.82	2.3	0.015	1.2
	Mo	4.01	0.7	0.015	1.2
723	N(O,C)	2.09	2.7	0.011	−1.3
	Mo	2.81	3.5	0.09	0.2
	Mo	4.03	1.8	0.009	0.8
NH_3 flow					
423	O	1.80	3.0	0.006	−0.8
	O	2.11	1.6	0.007	−0.8
	Mo	3.39	2.1	0.006	0.9
	N(O,C)	2.02	2.5	0.007	0.4
523	N(O,C)	2.13	2.2	0.007	0.4
	Mo	2.55	1.3	0.008	0.5
	N(O,C)	2.08	4.0	0.012	−2.2
673	Mo	2.82	1.9	0.012	−1.0
	Mo	3.99	1.3	0.012	−1.4
	N(O,C)	2.10	4.4	0.012	0.9
723	Mo	2.83	4.5	0.010	0.1
	Mo	4.01	2.35	0.009	1.0

[a] Coordination number. For crystalline compounds with asymmetric coordination sphere EXAFS CN represent average apparent values.

Another contribution to the decrease of the apparent CN values comes from the small size of particles as discussed earlier for Mo_2N and for relevant carbide Mo_2C [32,33]. Deconvolution of static disorder and size effects is a challenging task and lies beyond the scope of this work. Qualitatively, however, it can be seen that disorder increases from 523 to 673 K and then at 773 K the solids become again more ordered. Another conclusion from the EXAFS study is that transition to Mo_2N and ordering occur at slightly lower temperatures in ammonia than in N_2 flow (see Table 3).

As follows from the comparison of thermal analysis and EXAFS data, the initial stages of decomposition of **I** do not depend on the gas used, being common for the treatments in hydrogen, ammonia, and nitrogen. The resulting intermediate solid product is an amorphous compound $MoO_xC_yN_z$, with *x*, *y* and *z* coefficients depending on the temperature and on the gas flow applied. In all cases, auto reduction of the HMTA complex occurs leading to the decrease of the oxidation state from Mo(VI) in the initial complex to Mo(IV) in MoO_2 or Mo(II) in the nitrides and carbides.

3.3. Qualitative thermodynamical considerations.

To give a rationale of the observed effects, simple thermodynamical consideration might be relevant, as follows. Formally, multiple reactions can be written down for the decomposition of **I,** leading to carbide or nitride, e.g.

$$Mo_7O_{24}C_{12}H_{40}N_{12} \Rightarrow 7/2Mo_2C + 17/2CO + 31/2H_2O + 3NH_3 + 9/2N_2 \quad (1)$$

$$Mo_7O_{24}C_{12}H_{40}N_{12} \Rightarrow 7/2Mo_2N + 12CO + 12H_2O + 16/3NH_3 + 1/4N_2 \quad (2)$$

Unfortunately thermodynamic parameters of **I** are not available and therefore we cannot calculate precise equilibrium constants

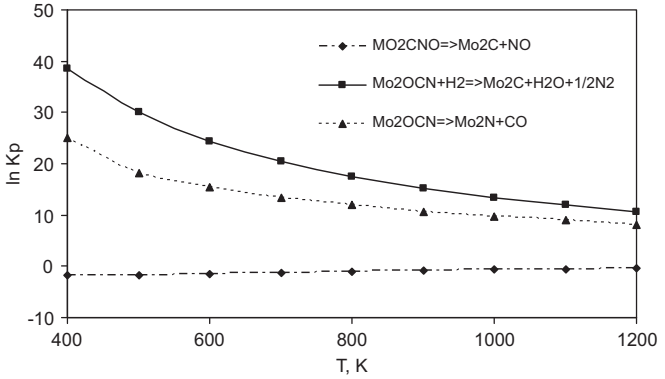

Fig. 10. Relative equilibrium constants for **I** decomposition leading to different products.

for such reactions. However we have demonstrated above that near 673 K the reactions of **I** in different gases pass through a common amorphous intermediate state $Mo_2C_xN_yO_z$ with *x* and *y* coefficients close to 1, further approximately designed as Mo_2CNO. Therefore we can tentatively neglect low-temperature part of evolution, and consider the final composition as being determined only by evolution of the Mo_2CNO solid above 673 K. Thermodynamical properties of this amorphous intermediate are unknown as well as those of **I**. However it can be considered as zero level reference to compare further reactions, leading to the products with known properties. At this level of approximation, comparison is possible of relative free energy of different decomposition reactions,

$$Mo_2CNO \Rightarrow Mo_2N + CO \quad (3)$$

$$Mo_2CNO + H_2 \Rightarrow Mo_2C + H_2O + 1/2N_2 \quad (4)$$

$$Mo_2CNO \Rightarrow Mo_2C + NO \quad (5)$$

Note that its exact stoichiometry does not play any role for our discussion, but only the nature of the products. Comparison of the equilibrium constants of reactions (3–5) reduces therefore to comparison of free formation energy of the products.

The equilibrium constants Kp of reactions (3–5) are presented in Fig. 10. Obviously, within the whole range of temperatures, under the inert atmosphere formation of nitride is favorable, whereas under hydrogen flow carbide becomes energetically preferred product, as observed in the experiment. This can be also expected from common chemical sense: hydrogen allows oxygen to be removed as water, increasing the probability for carbon to stay within the solid. In other terms, for the amorphous Mo_2OCN precursor to decompose thermally towards Mo_2C carbide, two of more electronegative light elements (N, O) must leave it and one less electronegative (C) must stay within the solid. In the absence of external reducing agents, this way would require formation of nitrogen oxides or such counterintuitive processes as release of molecular oxygen from a low-oxidation state Mo compound.

As with switching from the Mo_2N to MoO_2 product in the presence of water is quite straightforward and depends on the equilibrium of reaction (6), which is obviously shifted to the left by water and to the right by ammonia.

$$Mo_2N + 2H_2O = MoO_2 + 1/2H_2 + NH_3 \quad (6)$$

3.4. Catalytic properties

Though the obtained materials might find various applications, our activity was primarily directed on their catalytic use, namely

on the hydrotreating reactions. For binary Mo_2N there is a sufficient evidence that under hydrotreating conditions molybdenum sulfide MoS_2 forms on the surface of nitride, which then controls its catalytic properties [34]. The idea was therefore to obtain unsupported catalysts, containing Mo_2N core and active MoS_2 phase supported on it. Due to extreme thermal stability of Mo_2N one can expect obtaining high specific surface areas and thermally stable catalysts. The properties of the catalysts prepared under N_2 flow are discussed in detail in our recent work [35]. Here we focus on the difference between Mo_2N prepared from **I** under nitrogen and under ammonia flow.

Thiophene HDS was studied for two series of solids decomposed in N_2 and in NH_3, having reasonably high values of Ssp. In most experiments, freshly prepared nitride samples were directly introduced to the catalytic test. However for the solids obtained at 823 K and at 923 K another type of pre-treatment was applied in which freshly prepared nitride was first treated with H_2S/H_2 at 673 K for 4 h and then introduced to the HDS test.

All the solids were studied in thiophene HDS for 48 h. During the first 16 h considerable evolution of the HDS activity occurred and then the activity changed only negligibly, the catalyst being at the steady state (note, however, that more long-term deactivation might occur at the weeks or months scale, but this question is beyond the scope of our paper). The steady state rates of thiophene HDS at 523 K (Fig. 11) show that the dependence of HDS activity on the treatment temperature has a (smooth) maximum for both treating gases. This maximum is placed at lower temperature for NH_3 and the corresponding maximal HDS activity is higher. More important, however, is the difference between the solids sulfided with H_2S/H_2 mixture. For such sulfided solids, the N_2-issued samples demonstrated a drastic drop of HDS rate, whereas the activity of NH_3-issued catalysts considerably increased after sulfidation. The most active catalysts were obtained from the decomposition under ammonia flow at relatively low temperature (823 K), followed by sulfidation. In this case the specific mass activity was several times higher than that for the MoS_2 reference catalyst obtained from ammonium thiomolybdate (used as a benchmark for the performance of unsupported catalysts, see [36]).

Chemical analysis (Table 2) and specific surface area measurements (Fig. 12) suggest that the maximum of HDS activity is observed apparently due to the result of two processes, which have the opposite influence. The increase of the treatment temperature allows preparing more pure nitrides, thus improving HDS activity. On the other hand it leads to gradual sintering. As follows from Fig. 12, heating of **I** under NH_3 flow at relatively low

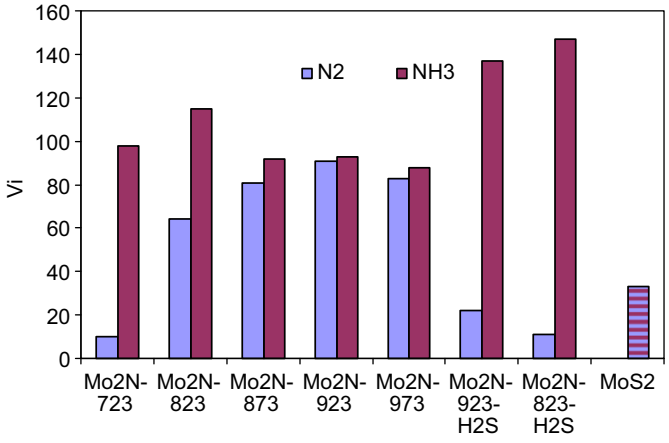

Fig. 11. Thiophene HDS rate (10^{-8} mol $g^{-1}s^{-1}$) for the solids prepared under different conditions under N_2 and under NH_3 atmosphere.

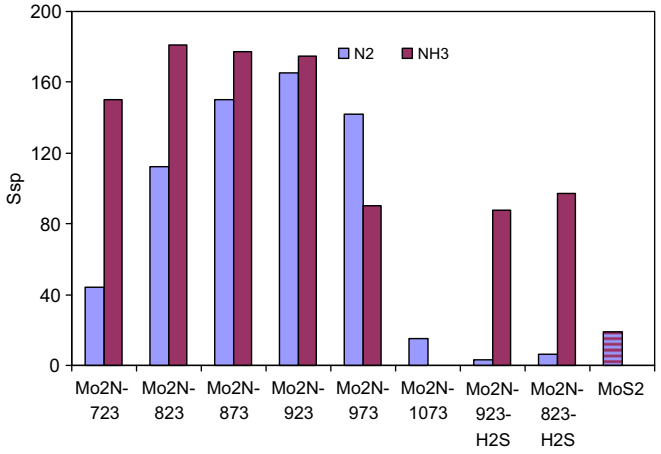

Fig. 12. Specific surface area for the solids prepared under different conditions under N_2 and under NH_3 atmosphere.

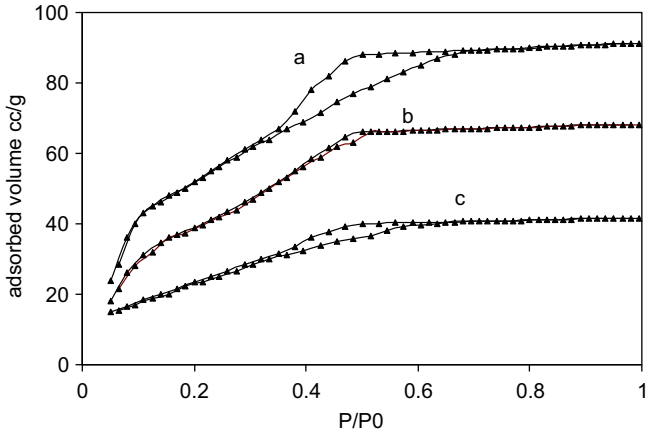

Fig. 13. Nitrogen adsorption–desorption isotherms for the solids obtained from decomposition of **I** at 923 K under NH_3 (a); under N_2 (b) and the solid (a) after sulfidation with H_2S/H_2 mixture at 673 K (c).

temperatures yields materials with high Ssp. However there is no direct proportionality between Ssp and HDS activities. In the series of solids treated under N_2 and under NH_3, the latter demonstrated better HDS catalytic activity even for somewhat lower Ssp (cf. samples obtained at 973 K).

Two additional advantages of the NH_3 treatment can be indicated. First, ammonia-treated solids demonstrated better porosity. Thus, NH_3-issued solid Mo_2N-823 had pore volume of 0.17 cm^3/g with a hysteresis loop in the mesoporosity range (Fig. 13a). At the same time the N_2-treated samples were essentially microporous with virtually no hysteresis loop in the mesopores region, their pore volume being difficult to measure (Fig. 13b). Obviously, during further treatment or during the catalytic reaction, the pores of N_2-treated solids should be easily clogged. Most strikingly this difference reveals in the sulfided samples. After sulfidation with the H_2S/H_2 mixture the specific surface area of N_2-treated samples drops down drastically to several units of m^2/g. In contrast to N_2-treated solid, sulfidation of γ-Mo_2N obtained in NH_3 at 823 K (181 m^2/g) lead to a material with high surface area (97 m^2/g) and still appreciable pore volume of 0.09 cm^3/g.

The second point of difference follows already from the data of chemical analysis but was additionally supported by the XPS study. From Table 2 it can be concluded that the treatment with N_2 necessitates higher temperatures to obtain relatively pure

nitride than heating in NH_3. Carbon and oxygen remain in such solids as impurities, but their amount at the surface might be high and might hinder catalytic activity by polluting the surface. The state of these impurity elements is not well defined but seemingly they form amorphous oxycarbonitride matter. Comparison of the XPS spectra of N_2- and NH_3-treated solids illustrates this point, as follows.

Table 4
Surface composition of three solids prepared under different conditions, as determined from the analysis of XPS spectra (all numbers correspond to per cent surface concentrations).

Treatment conditions (K)	C	O	S	Mo			
				Total	$Mo^{\delta+}$[a]	Mo (IV)[a]	Mo (VI)[a]
N_2, 823	36	28	–	36	40	16	44
NH_3, 823	18	16	–	65	67	19	14
NH_3, 823 H_2/H_2S, 673	17	8	27	57	81[b]	12	7

[a] In % of total molybdenum.
[b] Binding energy of Mo(IV) in sulfide is significantly lower than in oxide (cf. Fig. 13).

The amounts of the elements on the surface as determined from XPS are presented in Table 4. The corresponding Mo 3*d* spectra are shown in Fig. 14. Despite some uncertainty brought by device-issued carbon, it can be stated that much higher concentration of carbon was present on the surface of N_2-treated Mo_2N solids than for the NH_3-treated ones. At the same time high oxidation states of molybdenum were more abundant in the N_2-treated solid. While oxygen can be easily replaced by sulfur during further sulfidation, carbon impurity for such materials might be more resistant and hinder HDS activity.

The Mo 3*d* XPS doublets were analyzed using an intensity ratio of 2/3 and a splitting of 3.2 eV. Binding energy (BE) was attributed to Mo oxidation states on the basis of previous XPS studies [37,38]. Our XPS results show the presence of several forms of Mo on the surface. In the initial Mo_2N, three types of molybdenum were observed with BE 228.5, 230.0 and 231.9 eV, corresponding to Mo_2N (more generally, to $Mo^{\delta+}$ $2 \le \delta < 4$, [39]) or MoS_2; Mo(IV) oxide and Mo(VI) oxide species, respectively. After sulfidation treatments, the relative amount of Mo(VI) and Mo(IV) oxide species decreased. Though the values of BE for $Mo^{\delta+}$ and Mo(IV) sulfide (228.7 eV) are too close to be deconvoluted reliably, the decrease of the amount of oxide species and simultaneous increase of the sulfur content allow concluding that

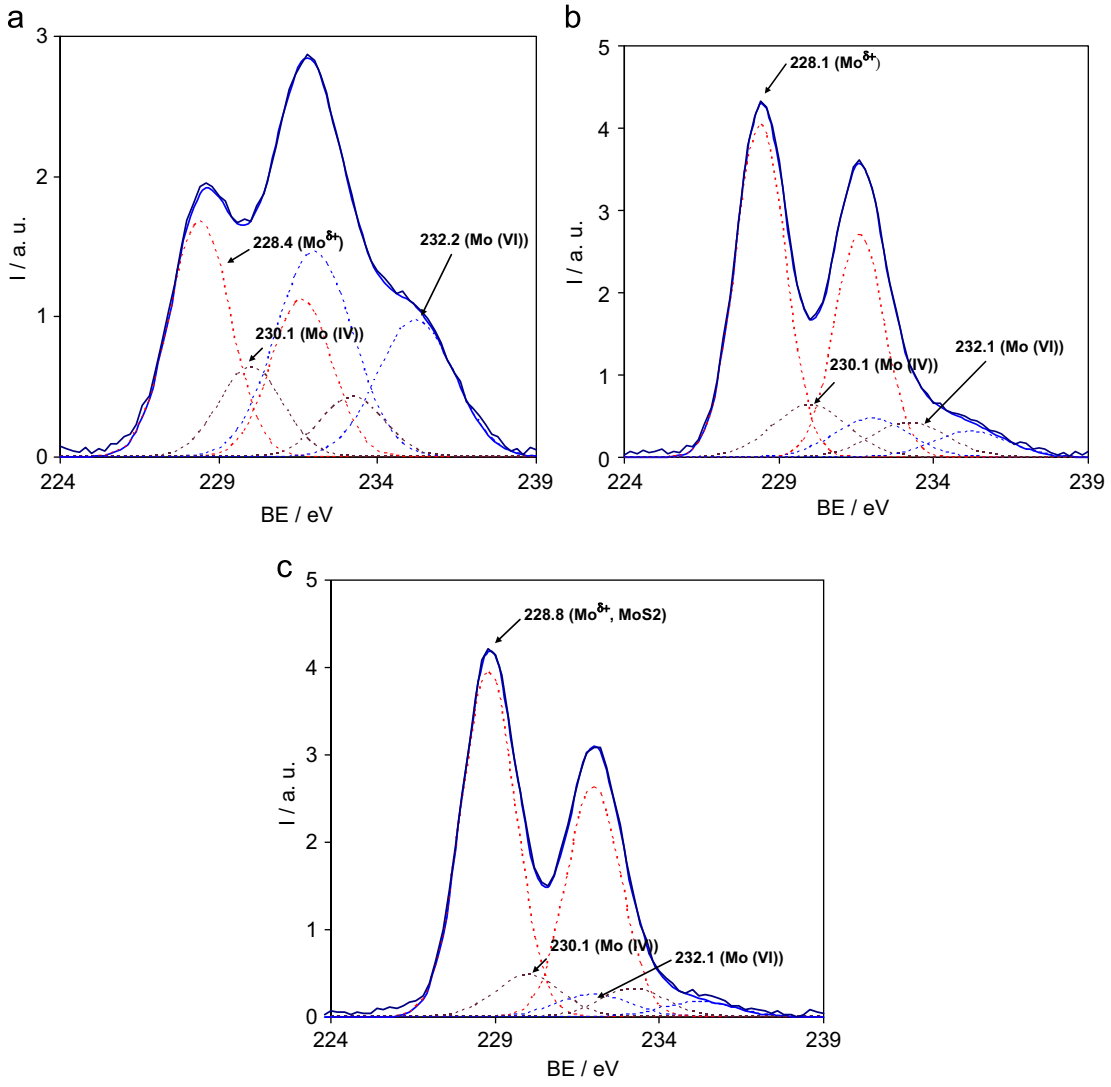

Fig. 14. XPS spectra of Mo_2N obtained from **I** at 823 K under nitrogen (a), under NH_3 (b) and the solid (b) after sulfidation with H_2S/H_2 mixture at 673 K (c).

sulfidation occurs by transformation of oxide species to MoS_2 (Fig. 14c).

Relatively poor catalytic activity of the Mo_2N catalyst prepared from **I** under nitrogen was recently observed in [40] for toluene hydrogenation reaction. It finds an obvious explanation in the results of the present study.

4. Conclusions

In summary, decomposition of heptamolybdate–HMTA complex **I** may lead to dispersed nitride, carbide or oxide materials. The nature of obtained products can be controlled by gas atmosphere and temperature. The preparation technique is very simple and in the case of nitrides allows lowering preparation temperature and obtaining materials with high specific surface areas. In situ EXAFS, chemical analysis and thermal analysis show that below 673 K similar decomposition steps occur independently on the nature of the gas atmosphere, leading to amorphous Mo intermediate material, which further evolves to nitride, carbide or oxide. The high temperature part of evolution depends crucially on the nature of gas flow.

The most interesting materials for the catalytic applications were obtained under nitrogen or ammonia flow. Highly dispersed molybdenum nitride was obtained in both cases. However the solids treated with ammonia show better textural properties and lower contents of impurities on the surface than the solids prepared under N_2 flow. Moreover, crystallized Mo_2N material can be obtained under NH_3 flow already at 823 K whereas at least 923 K is needed under N_2 flow.

Nitride-based solids were compared in the model thiophene HDS reaction. Our previous results and literature data show that the active phase in HDS is not the nitride itself, but MoS_2 formed on the surface of nitride particles. Sulfidation with the reaction mixture or with hydrogen sulfide allows obtaining active catalysts containing nitride core and sulfide surface layer. These materials have high specific surface, which provide sulfide catalysts more active than conventional unsupported sulfide. The optimal preparation conditions obtained in this work include treatment with NH_3 at 823 K followed by sulfidation with H_2S/H_2 mixture at 673 K.

No optimization of Mo_2C carbide properties has been carried out in this work. However the results obtained for decomposition of **I** in hydrogen diluted with a non-reactive gas show that the textural properties of carbide can be also significantly improved by varying the preparation conditions. Another promising direction where the approach described here can be applied seems to be preparation of supported nitrides. Indeed, the complex **I** is relatively well soluble in water. It can therefore be deposited via impregnation on a (mesoporous) support. Subsequent treatment with NH_3 under soft conditions might represent an interesting way for preparing highly dispersed supported Mo_2N catalysts.

Acknowledgments

We thank especially HASYLAB staff for help in the EXAFS measurements. In particular, M. Herrmann. P. Kappen at beamline X1 and the safety group at HASYLAB are gratefully acknowledged for their support and the constructive discussion of the safety aspects.

References

[1] L. Volpe, M. Boudart, J. Solid State Chem. 59 (1985) 332–347.
[2] L. Volpe, M. Boudart, J. Solid State Chem. 59 (1985) 348–356.
[3] J.S. Lee, S.T. Oyama, M. Boudart, J. Catal. 106 (1987) 125–133.
[4] S.T. Oyama, Catal. Today 15 (1992) 179–200.
[5] J. Trawczynski, Appl. Catal. A 197 (2000) 289–293.
[6] M. Nagai, Appl. Catal. A 322 (2007) 178–190.
[7] J.S. Choi, G. Bugli, G. Djéga-Mariadassou, J. Catal. 193 (2000) 238–247.
[8] P. Da Costa, J.L. Lemberton, C. Potvin, J.M. Manoli, G. Perot, M. Breysse, G. Djega-Mariadassou, Catal. Today 65 (2001) 195–200.
[9] D. Mckay, J.S.J. Hargreaves, J.L. Rico, J.L. Rivera, X.L. Sun, J. Solid State Chem. 181 (2008) 325–333.
[10] R. Kojima, K.I.R. Aika, Chem. Lett. (2000) 514–515.
[11] J. Monnier, H. Sulimma, A. Dalai, G. Caravaggio, Appl. Catal. A 382 (2010) 176–180.
[12] E. Puello-Polo, J.L. Brito, Catal. Today 149 (2010) 316–320.
[13] A.C.L. Gomes, M.H.O. Nunes, V. Teixeira da Silva, J.L.F. Monteiro, Study Surf. Sci. Catal. 154 (2004) 2432–2440.
[14] K.S. Suslick, T. Hyeon, M. Fang, Chem. Mater. 8 (1996) 2172–2179.
[15] J.D. Wu, C.Z. Wu, Z.M. Song, F.M. Li, Thin Solid Films 311 (1997) 62–66.
[16] Z.W. Yao, J. Alloys Comp. 475 (2009) L38–L41.
[17] P. Afanasiev, Inorg. Chem. 41 (2002) 5317–5318.
[18] S. Chouzier, P. Afanasiev, M. Vrinat, T. Cseri, M. Roy-Auberger, J. Solid State Chem. 179 (2006) 3314–3323.
[19] S. Chouzier, P. Afanasiev, M. Vrinat, T. Cseri, M. Roy-Auberger, Prep. Am. Chem. Soc., Div. Petr. Chem. 51 (2006) 285–287.
[20] H. Wang, W. Li, M. Zhang, Chem. Mater. 17 (2005) 3262–3267.
[21] H.M. Wang, X.H. Wang, M.H. Zhang, X.Y. Du, W. Li, K.Y. Tao, Chem. Mater. 19 (2007) 1801–1807.
[22] P. Afanasiev, S. Chouzier, T. Czeri, G. Pilet, C. Pichon, M. Roy-Auberger, M. Vrinat, Inorg. Chem. 47 (2008) 2303–2311.
[23] Z.W. Yao, L. Wang, H. Dong, J. Alloys Compd. 473 (2009) L10–L12.
[24] G. Horvath, K. Kawazoe, J. Chem. Eng. Japan 16 (1983) 470–475.
[25] C. Geantet, Y. Soldo, C. Glasson, N. Matsubayashi, M. Lacroix, O. Proux, O. Ulrich, J.L. Hazemann, Catal. Lett. 73 (2001) 95–98.
[26] R.E. Jentoft, S.E. Deutsch, B.C. Gates, Rev. Sci. Instrum. 67 (1996) 2111–2112.
[27] A.L. Ankudinov, C.E. Bouldin, J.J. Rehr, J. Sims, H. Hung, Phys. Rev. B 65 (2002) 104–107.
[28] K.V. Klementev, J. Phys. D 34 (2001) 209–217.
[29] M.A. Tsurov, P.V. Afanasiev, V.V. Lunin, Appl. Catal. 15 (1993) 205–221.
[30] C. Thomazeau, P. Afanasiev, V. Martin, Appl. Catal. 199 (2000) 61–72.
[31] D. Genuit, P. Afanasiev, M. Vrinat, J. Catal. 235 (2005) 302–317.
[32] Z.-L. Liu, M. Meng, Y.-L. Fu, M. Jiang, T.-D. Hu, Y.-N. Xie, T. Liu, Mater. Lett. 54 (2002) 364–371.
[33] A.S. Rocha, V. Teixeira da Silva, J.G. Eon, S.M.C. Menezes, A.C. Faro Jr., A.B. Rocha, J. Phys. Chem. B 110 (2006) 15803–15811.
[34] U.S. Ozkan, L. Zhang, P.A. Clark, J. Catal. 172 (1997) 294–306.
[35] S. Chouzier, T. Czeri, M. Roy-Auberger, M. Vrinat, P. Afanasiev, Appl. Catal. A 400 (2011) 82–90.
[36] P. Afanasiev, C. R. Chim. 11 (2008) 159–182.
[37] R.B. Quincy, M. Houalla, A. Proctor, D.M. Hercules, J. Phys.Chem. 94 (1990) 1520–1526.
[38] K. Hada, M. Nagai, S. Omi, J. Phys. Chem. B 104 (2000) 2090–2098.
[39] M. Ymada, J. Yasumaru, M. Houalla, D.M. Hercules, J. Phys. Chem. 95 (1991) 7037–7042.
[40] M.L. Frauwallner, F. López-Linares, J. Lara-Romero, C.E. Scott, V. Ali, E. Hernández, P. Pereira-Almao, Appl. Catal. 394 (2011) 62–70.